

Multi-decadal variations in Southern Hemisphere atmospheric

¹⁴C: Evidence against a Southern Ocean sink at the end of the

Little Ice Age CO₂ anomaly

Chris S.M. Turney^{1*}, Jonathan Palmer¹, Alan Hogg², Christopher J. Fogwill¹, Richard Jones³,
Christopher Bronk Ramsey⁴, Pavla Fenwick⁵, Pauline Grierson⁶, Janet Wilmshurst^{7,8}, Alison
O'Donnell⁶, Zoë Thomas¹ and Mathew Lipson¹

¹Climate Change Research Centre and School of Biological, Earth and Environmental Sciences, University of New South Wales, Australia; ²Waikato Radiocarbon Laboratory, University of Waikato, Private Bag 3105, Hamilton, New Zealand; ³Department of Geography, Exeter University, Devon, EX4 4RJ, United Kingdom; ⁴Research Laboratory for Archaeology and the History of Art, University of Oxford, Dyson Perrins Building, South Parks Road, Oxford OX1 3QY, UK; ⁵Gondwana Tree-Ring Laboratory, P.O. Box 14, Little River, Canterbury 7546, New Zealand; ⁶Ecosystems Research Group, School of Plant Biology, The University of Western Australia, Crawley, Western Australia, Australia; ⁷Landcare Research, PO Box 40, Lincoln 7640, New Zealand; ⁸School of Environment, University of Auckland, Private Bag 92019, Auckland 1142, New Zealand.

*To whom correspondence may be addressed. Email: c.turney@unsw.edu.au.

This article has been accepted for publication and undergone full peer review but has not been through the copyediting, typesetting, pagination and proofreading process which may lead to differences between this version and the Version of Record. Please cite this article as doi: 10.1002/2015GB005257

Abstract

Northern Hemisphere-wide cooling during the Little Ice Age (LIA; CE 1650-1775) is associated with a ~ 5 ppmv decrease in atmospheric carbon dioxide. Changes in terrestrial and ocean carbon reservoirs have been postulated as possible drivers of this relatively large shift in atmospheric CO_2 , potentially providing insights into the mechanisms and sensitivity of the global carbon cycle. Here we report decadal-resolved radiocarbon (^{14}C) levels in a network of tree rings series spanning CE 1700-1950 located along the northern boundary of, and within, the Southern Ocean. We observe regional dilutions in atmospheric radiocarbon (relative to the Northern Hemisphere) associated with upwelling of $^{14}\text{CO}_2$ -depleted abyssal waters. We find the inter-hemispheric ^{14}C offset approaches zero during increasing global atmospheric CO_2 at the end of the LIA, with reduced ventilation in the Southern Ocean and a Northern Hemisphere source of old carbon (most probably originating from deep Arctic peat layers). The coincidence of the atmospheric CO_2 increase and reduction in the inter-hemispheric ^{14}C offset imply a common climate control. Possible mechanisms of synchronous change in the high latitudes of both hemispheres are discussed.

Keypoints

- Uncertainty over source of CO_2 during the end of the Little Ice Age (LIA)
- ^{14}C -dated Southern Hemisphere tree rings provide measure of ocean ventilation
- Southern Ocean upwelling suppressed suggesting a NH terrestrial source for CO_2

1. Introduction

Climate-carbon feedbacks are potentially a significant source of future warming [Cox *et al.*, 2000; Friedlingstein *et al.*, 2013; Gregory *et al.*, 2009; Meinshausen *et al.*, 2011], driven by changes in the natural sinks and sources of greenhouse gases [Collins *et al.*, 2013].

A major source of uncertainty is the oceanic response to future forcing [Friedlingstein *et al.*, 2013; Le Quéré *et al.*, 2009; Le Quéré *et al.*, 2007; Séférian *et al.*, 2012]. In the oceans, the dominant carbon sink today is widely considered to be the Southern Ocean [Bernardello *et al.*, 2014; Le Quéré *et al.*, 2007] but the dearth of continuous observations prior to the late twentieth century limits our understanding of regional contributions, how these may have changed over time and the mechanisms of change [Friedlingstein *et al.*, 2013; Landschützer *et al.*, 2015; Le Quéré *et al.*, 2009].

A potential way of extending historical observations of Southern Ocean air-sea carbon fluxes is the exploitation of atmospheric radiocarbon (^{14}C). Here deep water formation in the North Atlantic isolates surface water as part of the Meridional Overturning Circulation (MOC), most of which upwells in the Southern Ocean, induced by the strong, persistent westerly winds in the Southern Hemisphere [Marshall and Speer, 2012]. The slow pace of deep ocean circulation allows a sufficient amount of radioactive decay to significantly reduce radiocarbon activity of the abyssal waters, resulting in the upwelling (and outgassing) of “old” CO_2 on seasonal through to millennial timescales [Braziunas *et al.*, 1995; Galbraith *et al.*, 2011; Hogg *et al.*, 2013], depleting Southern Hemisphere atmospheric ^{14}C levels with a postulated change of 1‰ (8 ^{14}C years) per 10° of latitude [Braziunas *et al.*, 1995]. Whilst the longest observational record of atmospheric $^{14}\text{CO}_2$ is available from CE 1954 (Wellington, New Zealand) [Currie *et al.*, 2011], annually-resolved records of tree growth have a proven ability to preserve a passive measure of changing atmospheric radiocarbon, potentially

reaching back millennia [Turney and Palmer, 2007].

A period of particular interest for understanding past climate-carbon interactions is CE 1650 to 1775, during which time atmospheric CO₂ appears to have been ~5 ppmv below pre-CE 1650 levels [Ahn *et al.*, 2012; Cox and Jones, 2008; Etheridge *et al.*, 1996; Rubino *et al.*, 2013]. This slightly lower CO₂ appears associated with maximum cooling within a multi-centennial Northern Hemisphere-wide climatic downturn commonly described as the ‘Little Ice Age’ (LIA; CE 1250-1850) [Mann *et al.*, 2009; PAGES 2k Consortium, 2013]. The decrease and subsequent increase in atmospheric CO₂ provides a useful constraint on the century-timescale sensitivity of the carbon cycle to climate change [Cox and Jones, 2008]. While early observations raised the possibility the Southern Ocean may have been a driver behind these changes in atmospheric CO₂ [Trudinger *et al.*, 1999] recent work has suggested instead that Northern Hemisphere terrestrial sources were the primary cause, either through land use changes [Kaplan, 2015] or the vulnerability of deep Arctic peat layers to decay with warming towards the end of the LIA [Bauska *et al.*, 2015].

Here we investigate changes in the circulation of the Southern Ocean using decadal-resolved atmospheric radiocarbon levels within tree rings across the mid-latitudes of the Southern Hemisphere. Using ¹⁴C as a proxy of upwelling we test whether the Southern Ocean played a significant role in climate-carbon dynamics during the end of the LIA chronozone.

2. Methods

We collected wood samples for tree ring analysis at their southernmost growing limit along the northern fringes of, and within, the Southern Ocean: 1. *Callitris columellaris* from Lake Tay, Western Australia (33.03°S, 120.75°E) [Cullen and Grierson, 2009]; 2. *Libocedrus bidwillii* from Takapari Forest Park, North Island, New Zealand (40.07°S, 175.98°E) [Hogg *et al.*, 2002] 3. *Halocarpus biformis* from Doughboy Bay, Stewart Island, New Zealand

(47.47°S, 167.73°E); and 4. *Dracophyllum longifolium* from Northeast Harbour, Campbell Island, New Zealand (52.52°S, 169.22°E) (Figure 1). Each tree series formed part of a well-replicated, annually-resolved chronology with an ‘expressed population signal’ (or EPS) above 0.85, a threshold value commonly used to describe a robust, highly-replicated series [Briffa and Jones, 1990]. The Northeast Harbour *Dracophyllum longifolium* series did not extend all the way to CE 1700 and was only sampled to CE 1900. Supplementing these series are the reported radiocarbon measurements obtained from *Nothofagus dombeyi* in Tierra del Fuego, southern Chile (54°S, 71°W) [McCormac et al., 2002; Stuiver and Braziunas, 1998], from which decadal-averaged means were calculated up to CE 1850 (Table 1).

The tree ring series were decadal sampled from CE 1700 (to capture the latter part of the LIA chronozone) up to CE 1950 (immediately prior to the bomb spike) [Hua et al., 2013]. A cross-section (or biscuit) was cut and transported to the laboratory where a radial strip was removed for analysis and the residual offcuts archived. The radial strip was first dried and then sanded progressively stepping from coarse to fine grit paper until a highly polished surface was obtained. After this step, the radii were studied under a binocular microscope and the annual rings cross-dated and assigned a calendar year. Growth rings were then grouped according to decade (e.g., 1940-1949, 1930-1939 etc.) and bulk decadal samples collected by separating each decade of rings along a ring boundary by first making fine radial cuts with a band saw and then using a chisel. As such, the internal age incorporation for each sample is 10 years. For radiocarbon (^{14}C) dating, chemical pre-treatment of the bulked (decadal) wood samples resulted in the purification of alpha-cellulose – as this wood fraction is deemed the most reliable for minimizing potential contamination and providing the most robust ^{14}C ages required for such high-precision study [Hogg et al., 2006]. Alpha-cellulose extraction begins with an acid-base-acid pretreatment at 80 °C, with samples treated with 1N HCl for 60 min, followed by successive 30-min treatments with 1N

NaOH until the supernatant liquid remained clear, ending with another 60-min 1N HCl wash. Holocellulose was then extracted by using successive 30-min treatments of acidified NaClO₂ at 70°C until the wood shavings were bleached to a pale yellow colour. Alpha-cellulose was then prepared by a final treatment with NaOH followed by a further acid wash (1N HCl at 70°C for 30 min) and repeated washing with distilled water until a pH of >6 was achieved. Samples were then graphitised in the Waikato Radiocarbon Laboratory and measured for radiocarbon by accelerator mass spectrometry (AMS) at the University of California at Irvine (UCI). For the youngest samples (i.e., 1940-1950) an initial solvent extraction was added to remove mobile components (resins etc) thereby reducing the potential for 'bomb' ¹⁴C translocating across the ring boundaries. A major advantage of all samples being prepared in one laboratory (Waikato) and measured for ¹⁴C in a single facility (UCI) is the potential for inter-laboratory inconsistencies to be avoided, reducing the age uncertainties (Table 1).

Radiocarbon ages of the samples were compared to the Northern Hemisphere radiocarbon dataset (IntCal13) [Reimer *et al.*, 2013] using a Defined Sequence model (D_Sequence) [Bronk Ramsey and Lee, 2013] in OxCal 4.2. To accommodate the mean Southern Hemispheric offset, a Delta_R with the prior U(-10,90) was used (allowing a 50 year or 0.625% margin either side of 40 years or 0.5%). Using Bayes theorem, the algorithms employed sample possible solutions with a probability that is the product of the prior and likelihood probabilities. Taking into account the age model and the actual ¹⁴C age measurements, the posterior probability densities quantify the most likely age distributions and allowed us to estimate regional offsets to the Northern Hemisphere across common periods of time. To determine a time series of changing regional offsets to the Northern Hemisphere, the IntCal13 dataset was extracted at 0.5-year intervals from OxCal 4.2 and the mean decadal difference with weighted error calculated (Table 2). We then compared the weighted mean and standard deviations of both the IntCal13 and our Southern Hemisphere

series using a *t*-test of each pair of values at each decade. This was done to determine time periods when no significant difference occurred (i.e. no interhemispheric offset).

3. Results and Discussion

The new Southern Hemisphere tree-ring ^{14}C series record large offsets from the average Northern Hemisphere radiocarbon dataset IntCal13 [Reimer *et al.*, 2013]. For the common period of overlap (CE 1700-1850), the Takapari (North Island) ^{14}C measurements are statistically identical to the previously reported New Zealand Takapari-Hihitari ages produced by the University of Waikato (-3 ± 29 years) [Hogg *et al.*, 2002] providing confidence the dataset is comparable to SHCal13 [Hogg *et al.*, 2013] but offering greater sample depth over the last 300 years. Dividing the tree sequences into pre- and post-industrial periods, the larger offsets were recorded prior to CE 1850 at Lake Tay in Western Australia (57.0 ± 6.0 ^{14}C years) and Doughboy (Stewart Island; 44.4 ± 5.9 ^{14}C years) (Table 2); the smaller offsets were recorded at Takapari and Tierra del Fuego (southern Chile) at 37.7 ± 5.7 and 38 ± 2.6 ^{14}C years respectively. With industrialization, we observe a decrease in the offset, with Lake Tay (17.5 ± 6.5 ^{14}C years), Takapari (15.3 ± 6.2 ^{14}C years) and Doughboy (25.0 ± 6.6 ^{14}C years) all recording a marked decline after CE 1850. In the time period captured by Northeast Harbour, Campbell Island (CE 1900-1950), the subantarctic series preserves the greatest offset to IntCal13, with a difference of 30.2 ± 9.3 ^{14}C years.

Two important points can be made from the above observations. First, there is no obvious Southern Hemisphere latitudinal ^{14}C gradient [Braziunas *et al.*, 1995]. Whilst Campbell Island (53°S) exhibits the largest of all the ^{14}C offsets from the Northern Hemisphere, Tierra del Fuego, which is at a similar high-latitude (54°S) shows one of the smallest offsets and Lake Tay, which is at a much lower latitude (33°S) shows relatively old ages. Second, regional offsets in Southern Hemisphere atmospheric radiocarbon are

measurable, though whether this is due to differences in the growing seasons (as suggested for the Northern Hemisphere) [Bronk Ramsey *et al.*, 2010; Manning *et al.*, 2001] is presently unclear. We therefore concentrate on the temporal variations preserved across the datasets.

Previous work has indicated that temporal variability in Southern Hemisphere atmospheric ^{14}C is strongly influenced by sea ice extent in the Southern Ocean but with the potential for regional differences [Braziunas *et al.*, 1995]. To investigate multi-decadal to centennial changes in the atmospheric radiocarbon offset, we compare the mean of Southern Hemisphere ^{14}C ages with the IntCal13 Northern Hemisphere record [Reimer *et al.*, 2013] (Figure 2). Although the long-term trend is most probably a result of industrialization and a greater emission of fossil fuels (dead- ^{14}C) in the Northern Hemisphere from CE 1850 [Ahn *et al.*, 2012; McCormac *et al.*, 1998], at least two prominent reductions in the offsets appear to be recorded; a *t-test* between the data-points of the two series shown in Figure 2 identified the periods CE 1780-1800, 1860-70 and possibly post 1930 (Figures 2 and 3; gray shaded columns). Similar periods when the offset converged on zero have also been suggested for New Zealand during CE 1725-1795 and 1805-1865 [McCormac *et al.*, 1998], the timing of which is consistent with our wider Southern Hemisphere results. The sustained nature of these multi-decadal fluctuations in the tree-ring series suggests a natural, time-varying component in the atmospheric ^{14}C content may be operating in the Southern Hemisphere.

To explore the observed changes in more detail (independent of differences in the growing season across the network of sites), we generated individual time series of the mean decadal difference (offset) to IntCal13 for each record (Figure 3). Offsets are observed among the different ^{14}C datasets but importantly there is a remarkable degree of coherence in temporal variability between the different sites (Figure 3), implying changes in the flux of old carbon to the atmosphere. Fitting a locally weighted smoothing (LOESS) curve to the individual series identifies a long-term trend towards a negligible offset between our study

regions and IntCal13 [Reimer *et al.*, 2013]. The greatest change is observed at Lake Tāu where the offset declines from a maximum value of ~83 ^{14}C years (CE 1700-1710) to ~28 ^{14}C years across CE 1790-1800.

Importantly, the collapses in ^{14}C offset to the Northern Hemisphere centred on CE 1790 and 1860 are observed in all our records, indicating the shifts were Southern Hemisphere-wide, and not region-specific. The ~60 year recurrence interval of interhemispheric collapse may be linked to the 120-130 year periodicity in UK-NZ ^{14}C differences [Hogg *et al.*, 2011] suggested to be driven by changes in sea ice extent and wind speed [Braziunas *et al.*, 1995] or as recent studies have proposed, changes in the latitude of core flow [Rodgers *et al.*, 2011] over the Southern Ocean. A poleward shift in westerly airflow over the Southern Hemisphere has been found to enhance northward Ekman transport of cool Antarctic surface waters, drawing up more carbon-rich (^{14}C -depleted) subsurface waters south of the Antarctic Circumpolar Current (ACC) [Galbraith *et al.*, 2011; Landschützer *et al.*, 2015; Le Quéré *et al.*, 2007] implying there may be an association with atmospheric CO_2 . We do observe a relationship between ^{14}C and CO_2 but find the opposite to what we might expect at the end of the LIA chronozone; namely reductions in the offset coincide with increases in atmospheric CO_2 as recorded in the West Antarctic Ice Sheet (WAIS) Divide ice core [Bauska *et al.*, 2015] (Figure 3). Curiously, the ^{14}C offset at the Tierra del Fuego site is less variable than at other sites, showing limited expression across the CE 1790 event.

It is intriguing that changes in Southern Ocean ^{14}C coincide with inflections in the CO_2 record. Our Southern Hemisphere radiocarbon values, however, strongly argue against a Southern Ocean source for the increase in atmospheric carbon dioxide. The collapse in the ^{14}C offset centred on CE 1790 coincides with a maxima in Northern Hemisphere radiocarbon ages (Figure 2) at the same time as the observed global increase in atmospheric CO_2 [Ahn *et*

al., 2012] (Figure 3). Whilst anthropogenic changes across Northern Hemisphere landscapes have been proposed as a possible cause for the rise in CO₂ at the end of the LIA [*Kaplan*, 2015] it seems unlikely that the near-modern ¹⁴C values from carbon released from this source would be sufficient to drive the collapse in the observed interhemispheric offset [*Bauska et al.*, 2015; *Graven*, 2015]. The reduced offset centred on CE 1790 is more consistent with an old-carbon (¹⁴C-depleted) high-latitude terrestrial source, such as decaying peat [*Bauska et al.*, 2015]. However, no substantive change in Northern Hemisphere ¹⁴C are recorded across CE 1860, with relatively young ages across this period (Figure 2). Importantly, paleo-reconstructions indicate that alongside a warming climate post-LIA [*PAGES 2k Consortium*, 2013] there were highly variable changes in westerly airflow across the mid-latitudes of the Southern Hemisphere [*Lamy et al.*, 2010; *McGlone et al.*, 2010; *Turney et al.*, 2015] suggesting the Southern Ocean sea-air flux of ¹⁴CO₂ may play a role.

Alongside high-latitude Northern Hemisphere peatlands, the tropics have also been acknowledged as providing a possible source of carbon around the time of the LIA [*Bauska et al.*, 2015]. The strongest response of carbon fluxes in the tropics over recent decades, however, is not directly due to temperature changes but circulation changes associated with the El Niño-Southern Oscillation (ENSO); during La Niña events and associated strong trade winds, cloud cover has been observed to decline across the low latitudes, increasing solar irradiance (a limiting factor on forest net primary productivity in the equatorial tropics) and carbon sequestration, impacting global atmospheric CO₂ [*Cleveland et al.*, 2015; *Nemani et al.*, 2003]. ENSO is known to impact changes in inter-hemispheric atmospheric radiocarbon via two key regions. First, in the tropics, La Niña events drive an increased flux of ¹⁴C-depleted CO₂-rich water into the atmosphere at low latitudes [*Feely et al.*, 1999; *Sutton et al.*, 2014] which as a result of an equatorwards migration of the Intertropical Convergence Zone (ITCZ) can decrease the inter-hemispheric radiocarbon difference [*Turney and Palmer*,

2007].

ENSO, however, is also known to have a significant influence on climate and oceanographic conditions over the high latitudes of the Southern Hemisphere [Turner, 2004]. Significant changes in the air-sea exchange of carbon have been reported over recent decades and are projected for the future [Landschützer *et al.*, 2015; Xue *et al.*, 2015; Yuan, 2004], linked to changes in the strength of westerly airflow and the balance between upwelling of ^{14}C -depleted Circumpolar Deep Water and temperature of surface waters [Bernardello *et al.*, 2014; de Lavergne *et al.*, 2014; Landschützer *et al.*, 2015; Majkut *et al.*, 2014]. During La Niña events, for instance, a poleward shift in the Polar Jet Stream (and associated surface westerly winds) in the South Pacific is associated with a low-pressure system in the Bellinghausen Sea and cooler surface waters as a result of increased Ekman transport across the mid-latitudes [Landschützer *et al.*, 2015; Yuan, 2004]; positive sea-ice feedbacks further enhance regional cooling during these times (with the opposite association in the Weddell Sea) [Bertler *et al.*, 2004; Latif *et al.*, 2013; Yuan, 2004], reducing the sea-air flux of $^{14}\text{CO}_2$ to the Southern Hemisphere atmosphere. Given this relationship, our results imply there was a change in the pervasive ENSO state around CE ~1790 and 1860, with more La Niña-like events on multidecadal timescales, resulting in an poleward shift (or strengthening) of westerly winds across the South Pacific, reducing ocean ventilation across the region. This inference is consistent with reconstructed decreases in ENSO variance during these periods [Li *et al.*, 2013]. If the South Pacific is indeed a major driver of changes in the ‘interhemispheric’ gradient, it may explain the relatively low temporal variability of Chilean ^{14}C , with the Polar Jet Stream redirected north in the southeast Pacific, effectively bypassing Tierra del Fuego [Yuan, 2004].

4. Conclusions

Recent work has suggested the global increase in atmospheric CO₂ during the termination of the Little Ice Age was driven by enhanced decay of peatlands in the Northern Hemisphere. An alternative source of carbon may have been the Southern Ocean. Here we use a network of absolutely-dated tree ring series from across the mid-latitudes of the Southern Hemisphere to measure atmospheric radiocarbon as a proxy of upwelling of ¹⁴C-depleted abyssal waters. We find coincident regional collapses in the ¹⁴C offset to the Northern Hemisphere for approximately 20 years centred on CE 1790, 1860 and possibly 1950. Reductions in the regional offset strongly argue against a Southern Ocean source for the increase in atmospheric carbon dioxide at the end of the Little Ice Age and are consistent with a Northern Hemisphere terrestrial source. Whilst a pervasive periodicity has previously been reported for the offset between New Zealand and the Northern Hemisphere, here we recognize these changes occur across most of the Southern Hemisphere. Our results suggest that alongside the long-term increase in CO₂ post-LIA, multi-decadal variability in the sea-air flux of carbon-rich (¹⁴C-depleted) subsurface waters may have been modulated by the El Niño-Southern Oscillation (ENSO). We find long-term variability is near constant over Tierra del Fuego (54°S), suggesting air masses are relatively well mixed. In marked contrast, Campbell Island lies at a comparable latitude (53°S) to Tierra del Fuego and exhibits the greatest ¹⁴C offset, offering considerable potential for future work to detect changes in Southern Ocean upwelling and the global carbon cycle since CE 1950.

5. Acknowledgements

Part of this work was undertaken during the Australasian Antarctic Expedition 2013-2014. CSMT, CF and PG acknowledge the support of the Australian Research Council (FL100100195, FT120100004 and DP130104156). We thank the New Zealand Department of Conservation for permission to undertake sampling on Campbell and Stewart Islands

(permit numbers: 37687-FAU and National Permit SO-29897-FLO, Southland Application No 1011/38). The data reported in this study are provided in Table 1 and also lodged on the National Oceanic and Atmospheric Administration Paleoclimatology Database (<https://www.ncdc.noaa.gov/data-access/paleoclimatology-data>). We thank the two anonymous reviewers for their constructive comments which improved the manuscript.

References

Ahn, J., E. J. Brook, L. Mitchell, J. Rosen, J. R. McConnell, K. Taylor, D. Etheridge, and M. Rubino (2012), Atmospheric CO₂ over the last 1000 years: A high-resolution record from the West Antarctic Ice Sheet (WAIS) Divide ice core, *Global Biogeochemical Cycles*, 26(2), GB2027.

Bauska, T. K., F. Joos, A. C. Mix, R. Roth, J. Ahn, and E. J. Brook (2015), Links between atmospheric carbon dioxide, the land carbon reservoir and climate over the past millennium, *Nature Geoscience*, 8(5), 383-387.

Bernardello, R., I. Marinov, J. B. Palter, E. D. Galbraith, and J. L. Sarmiento (2014), Impact of Weddell Sea deep convection on natural and anthropogenic carbon in a climate model, *Geophysical Research Letters*, 41(20), 7262-7269.

Bertler, N. A. N., P. J. Barrett, P. A. Mayewski, R. L. Fogt, K. J. Kreutz, and J. Shulmeister (2004), El Niño suppresses Antarctic warming, *Geophysical Research Letters*, 31(15), L15207.

Braziunas, T. F., I. Y. Fung, and M. Stuiver (1995), The preindustrial atmospheric ¹⁴CO₂ latitudinal gradient as related to exchanges among atmospheric, oceanic, and terrestrial reservoirs, *Global Biogeochemical Cycles*, 9(4), 565-584.

Briffa, K. R., and P. D. Jones (1990), Basic chronology statistics and assessment, in *Methods of Dendrochronology: Applications in the Environmental Sciences*, edited by E. R. Cook and L. A. Kairiukstis, pp. 137-152, Kluwer Academic, Norwell, Mass.

Bronk Ramsey, C., and S. Lee (2013), Recent and planned developments of the program OxCal, *Radiocarbon*, 55(2-3), 720-730.

Bronk Ramsey, C., M. W. Dee, J. M. Rowland, T. F. G. Higham, S. A. Harris, F. A. Brock, A. Quiles, E. M. Wild, E. S. Marcus, and A. J. Shortland (2010), Radiocarbon-based chronology for Dynastic Egypt, *Science*, 328(5985), 1554-1557.

Cleveland, C. C., P. Taylor, K. D. Chadwick, K. Dahlin, C. E. Doughty, Y. Malhi, W. K. Smith, B. W. Sullivan, W. R. Wieder, and A. R. Townsend (2015), A comparison of plot-based satellite and Earth system model estimates of tropical forest net primary production, *Global Biogeochemical Cycles*, 29(5), 626-644.

Collins, M., et al. (2013), Long-term climate change: projections, commitments and irreversibility, in *Climate Change 2013: The Physical Science Basis. Contribution of Working Group I to the Fifth Assessment Report of the Intergovernmental Panel on Climate Change*, edited by T. F. Stocker, D. Qin, G.-K. Plattner, M. Tignor, S. K. Allen, J. Boschung, A. Nauels, Y. Xia, V. Bex and P. M. Midgley, Cambridge University Press, Cambridge, UK.

Cox, P. M., and C. Jones (2008), Illuminating the modern dance of climate and CO₂, *Science*, 321, 1642-1643.

Cox, P. M., R. A. Betts, C. D. Jones, S. A. Spall, and I. J. Totterdell (2000), Acceleration of global warming due to carbon-cycle feedbacks in a coupled climate model, *Nature*, 408, 184-187.

Cullen, L. E., and P. F. Grierson (2009), Multi-decadal scale variability in autumn-winter rainfall in south-western Australia since 1655 AD as reconstructed from tree rings of *Callitris columellaris*, *Climate Dynamics*, 33, 433-444.

Currie, K., G. Brailsford, S. Nichol, A. Gomez, R. Sparks, K. Lassey, and K. Riedel (2011), Tropospheric ¹⁴CO₂ at Wellington, New Zealand: the world's longest record, *Biogeochemistry*, 104(1-3), 5-22.

de Lavergne, C., J. B. Palter, E. D. Galbraith, R. Bernardello, and I. Marinov (2014), Cessation of deep convection in the open Southern Ocean under anthropogenic climate change, *Nature Climate Change*, 4(4), 278-282.

Etheridge, D. M., L. P. Steele, R. L. Langenfelds, R. J. Francey, J. M. Barnola, and V. I. Morgan (1996), Natural and anthropogenic changes in atmospheric CO₂ over the last 1000 years from air in Antarctic ice and firn, *Journal of Geophysical Research: Atmospheres*, 101(D2), 4115-4128.

Feely, R. A., R. Wanninkhof, T. Takahashi, and P. Tans (1999), Influence of El Niño on the equatorial Pacific contribution to atmospheric CO₂ accumulation, *Nature*, 398(6728), 597-601.

Friedlingstein, P., M. Meinshausen, V. K. Arora, C. D. Jones, A. Anav, S. K. Liddicoat, and R. Knutti (2013), Uncertainties in CMIP5 climate projections due to carbon cycle feedbacks, *Journal of Climate*, 27(2), 511-526.

Galbraith, E. D., et al. (2011), Climate variability and radiocarbon in the CM2Mc Earth System Model, *Journal of Climate*, 24(16), 4230-4254.

Graven, H. D. (2015), Impact of fossil fuel emissions on atmospheric radiocarbon and various applications of radiocarbon over this century, *Proceedings of the National Academy of Sciences*.

Gregory, J. M., C. D. Jones, P. Cadule, and P. Friedlingstein (2009), Quantifying carbon cycle feedbacks, *Journal of Climate*, 22(19), 5232-5250.

Hogg, A. G., J. Palmer, G. Boswijk, and C. Turney (2011), High-precision radiocarbon measurements of the tree-ring dated wood from New Zealand: 200 BC-AD 950, *Radiocarbon*, 53(3), 529-542.

Hogg, A. G., F. G. McCormac, T. F. G. Higham, P. J. Reimer, M. G. L. Baillie, and J. G. Palmer (2002), High-precision radiocarbon measurements of contemporaneous tree-ring

dated wood from the British Isles and New Zealand: AD 1850-950, *Radiocarbon*, 44, 633-640.

Hogg, A. G., L. K. Fifield, C. S. M. Turney, J. G. Palmer, R. Galbraith, and B. M. (2006), Dating ancient wood by high sensitivity Liquid Scintillation Spectroscopy and Accelerator Mass Spectrometry - Pushing the boundaries, *Quaternary Geochronology*, 1, 241-248.

Hogg, A. G., et al. (2013), SHCal13 Southern Hemisphere calibration, 0–50,000 years cal BP, *Radiocarbon*, 55(4), 1889-1903.

Hua, Q., M. Barbetti, and A. Z. Rakowski (2013), Atmospheric radiocarbon for the period 1950–2010, *Radiocarbon*, 55(4), 2059-2072.

Kaplan, J. O. (2015), Holocene carbon cycle: Climate or humans?, *Nature Geosci*, 8(5), 335-336.

Lamy, F., R. Kilian, H. W. Arz, J.-P. Francois, J. Kaiser, M. Prange, and T. Steinke (2010), Holocene changes in the position and intensity of the southern westerly wind belt, *Nature Geoscience*, 3(10), 695-699.

Landschützer, P., et al. (2015), The reinvigoration of the Southern Ocean carbon sink, *Science*, 349(6253), 1221-1224.

Latif, M., T. Martin, and W. Park (2013), Southern Ocean sector centennial climate variability and recent decadal trends, *Journal of Climate*, 26(19), 7767-7782.

Le Quéré, C., M. R. Raupach, J. G. Canadell, G. Marland, and et al. (2009), Trends in the sources and sinks of carbon dioxide, *Nature Geoscience*, 2(12), 831-836.

Le Quéré, C., et al. (2007), Saturation of the Southern Ocean CO₂ sink due to recent climate change, *Science*, 316, 1735-1738.

Li, J., et al. (2013), El Niño modulations over the past seven centuries, *Nature Climate Change*, 3, 822-826.

Majkut, J. D., J. L. Sarmiento, and K. B. Rodgers (2014), A growing oceanic carbon uptake: Results from an inversion study of surface pCO₂ data, *Global Biogeochemical Cycles*, 28(4), 335-351.

Mann, M. E., Z. Zhang, S. Rutherford, R. S. Bradley, M. K. Hughes, D. Shindell, C. Ammann, G. Faluvegi, and F. Ni (2009), Global signatures and dynamical origins of the Little Ice Age and Medieval Climate Anomaly, *Science*, 326, 1256-1260.

Manning, S. W., B. Kromer, P. I. Kuniholm, and M. W. Newton (2001), Anatolian tree rings and a new chronology for the east Mediterranean Bronze-Iron ages, *Science*, 294, 2532-2535.

Marshall, J., and K. Speer (2012), Closure of the meridional overturning circulation through Southern Ocean upwelling, *Nature Geoscience*, 5(3), 171-180.

McCormac, F. G., P. J. Reimer, A. G. Hogg, T. F. G. Higham, M. G. L. Baillie, J. Palmer, and M. Stuiver (2002), Calibration of the radiocarbon time scale for the southern hemisphere: AD 1850-950, *Radiocarbon*, 44, 641-651.

McCormac, F. G., et al. (1998), Temporal variation in the interhemispheric ¹⁴C offset, *Geophysical Research Letters*, 25, 1321-1324.

McGlone, M. S., C. S. M. Turney, J. M. Wilmshurst, and K. Pahnke (2010), Divergent trends in land and ocean temperature in the Southern Ocean over the past 18,000 years, *Nature Geoscience*, 3, 622-626.

Meinshausen, M., T. Wigley, and S. Raper (2011), Emulating atmosphere-ocean and carbon cycle models with a simpler model, MAGICC6–Part 2: Applications, *Atmospheric Chemistry and Physics*, 11(4), 1457-1471.

Nemani, R. R., C. D. Keeling, H. Hashimoto, W. M. Jolly, S. C. Piper, C. J. Tucker, R. B. Myneni, and S. W. Running (2003), Climate-driven increases in global terrestrial Net Primary Production from 1982 to 1999, *Science*, 300(5625), 1560-1563.

PAGES 2k Consortium (2013), Continental-scale temperature variability during the past two millennia, *Nature Geoscience*, 6(5), 339-346.

Reimer, P. J., et al. (2013), IntCal13 and Marine13 radiocarbon age calibration curves 0–50,000 years cal BP, *Radiocarbon*, 55(4), 1869-1887.

Rodgers, K. B., et al. (2011), Interhemispheric gradient of atmospheric radiocarbon reveals natural variability of Southern Ocean winds, *Climates of the Past*, 7(4), 1123-1138.

Rubino, M., et al. (2013), A revised 1000 year atmospheric $\delta^{13}\text{C}$ -CO₂ record from Law Dome and South Pole, Antarctica, *Journal of Geophysical Research*, 118, 1-18.

Séférian, R., D. Iudicone, L. Bopp, T. Roy, and G. Madec (2012), Water mass analysis of effect of climate change on air–sea CO₂ fluxes: The Southern Ocean, *Journal of Climate*, 25(11), 3894-3908.

Stuiver, M., and T. F. Braziunas (1998), Anthropogenic and solar components of hemispheric ¹⁴C, *Geophysical Research Letters*, 25(3), 329-332.

Sutton, A. J., R. A. Feely, C. L. Sabine, M. J. McPhaden, T. Takahashi, F. P. Chavez, G. E. Friederich, and J. T. Mathis (2014), Natural variability and anthropogenic change in equatorial Pacific surface ocean pCO₂ and pH, *Global Biogeochemical Cycles*, 28(2), 131-145.

Trudinger, C. M., I. G. Enting, R. J. Francey, D. M. Etheridge, and P. J. Rayner (1999), Long-term variability in the global carbon cycle inferred from a high-precision CO₂ and $\delta^{13}\text{C}$ ice-core record, *Tellus*, 51B, 233-248.

Turner, J. (2004), The El Niño-Southern Oscillation and Antarctica, *International Journal of Climatology*, 24, 1-31.

Turney, C. S. M., and J. Palmer (2007), Does the El Niño-Southern Oscillation control the interhemispheric radiocarbon offset?, *Quaternary Research*, 67, 174-180.

Turney, C. S. M., R. T. Jones, C. Fogwill, J. Hatton, A. N. Williams, A. Hogg, J.

Palmer, and S. Mooney (2015), A 250-year periodicity in Southern Hemisphere westerly winds over the last 2600 year, *Climates of the Past Discussions*, 11, 2159-2180.

Xue, L., L. Gao, W.-J. Cai, W. Yu, and M. Wei (2015), Response of sea surface fugacity of CO₂ to the SAM shift south of Tasmania: Regional differences, *Geophysical Research Letters*, 42(10), 3973-3979.

Yuan, X. (2004), ENSO-related impacts on Antarctic sea ice: a synthesis of phenomenon and mechanisms, *Antarctic Science*, 16(04), 415-425.

Accepted Article



Figure 1: Location of tree ring ^{14}C series discussed in text, the West Antarctic Ice Sheet (WAIS) Divide ice core [Bauska *et al.*, 2015] and mean locations of the Subtropical and Polar fronts (red lines).

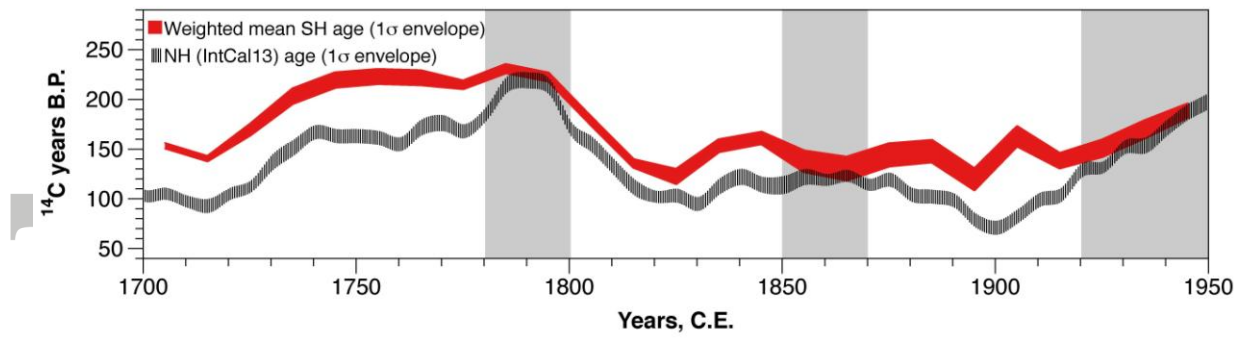


Figure 2: Weighted mean Southern Hemisphere atmospheric ^{14}C age (red envelope; 1σ range) compared to the Northern Hemisphere IntCal13 dataset (dashed black envelope; 1σ range) [Reimer *et al.*, 2013]. Gray columns denote periods discussed in text.

Accepted Article

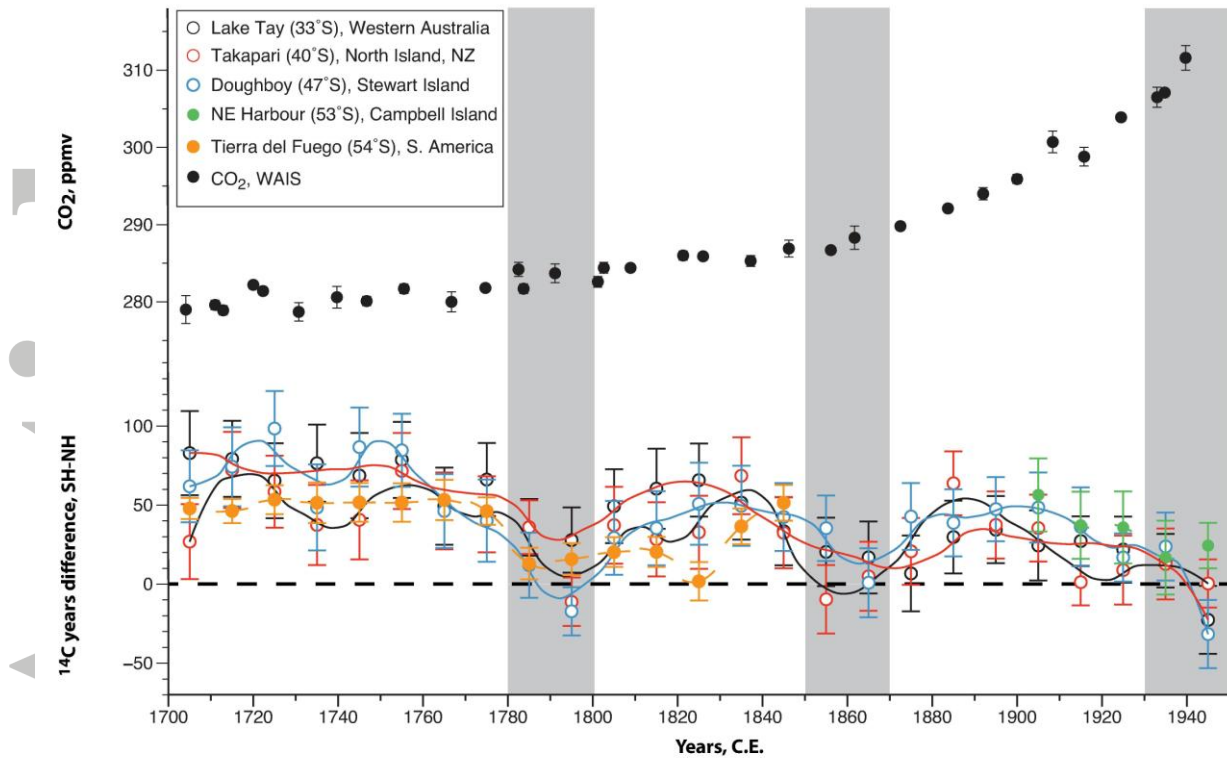


Figure 3: Decadal inter-hemispheric radiocarbon offsets calculated from the different tree ring series (colored circles) compared to the carbon dioxide (CO₂) concentration values (solid circles) inferred from the West Antarctic Ice Sheet (WAIS) Divide ice core [Bauska *et al.*, 2015]; WAIS data available at <http://ncdc.noaa.gov/paleo/study/18316>. A LOESS fit has been applied to each of the tree-ring ¹⁴C datasets. Gray columns denote common periods where the inter-hemispheric ¹⁴C offset approaches zero i.e. no offset between the hemispheres (dashed horizontal line).

Table 1: Decadal radiocarbon (^{14}C) ages for Southern Hemisphere tree ring series.

Years given as the mid-point of the dated decadal block. University of Waikato

laboratory numbers are denoted by 'Wk-'. * describe multiple samples used to calculate a weighted mean and age uncertainty. ¹Radiocarbon dataset previously reported for Tierra del Fuego [McCormac *et al.*, 2002; Stuiver and Braziunas, 1998]; multiple ages within each decade have been used to derive a weighted mean and age uncertainty.

Years C.E.	Lake Tay Wk-	Lake Tay ^{14}C $\pm 1\sigma$	Takapa ri, Wk-	Takap ari ^{14}C $\pm 1\sigma$	Doughb oy Wk-	Doughb oy ^{14}C $\pm 1\sigma$	Campb ell Island Wk-	Campb ell Island $^{14}\text{C} \pm 1\sigma$	Tierra del Fuego ¹ ^{14}C $\pm 1\sigma$
170 5	39764	188± 26	39564	132±2 3	39540	167±22			153± 3
171 5	39765	172± 23	39565	165±2 3	39541	167±24			139± 3
172 5	39766	177± 23	39566	170±2 2	39542	210±23			165± 7
173 5	39767	227± 23	39567	188±2 4	39543	199±26			202± 10
174 5	39768	232± 26	39568	204±2 4	39544	250±24			215± 10
175 5	39769	240± 23	39569	233±2 3	39545	246±22			213± 10
176 5	39770	220± 23	39570	217±2 3	39546	217±22			224± 10
177 5	39771	234± 22	39571	212±2 3	39547	208±25			214± 5
178 5	39772	249± 16	39572	249±1 5	39548	225±19			226± 6
179 5	39773	242± 19	39573	203±1 3	39549	197±13			230± 6
180 5	39587	205± 22	39574	193±2 3	39550	185±22			176± 5
181 5	39588	173± 24	39575	141±2 2	39551	148±22			133± 5

182		169±		136±2				105±
5	39589	22	39576	2	39552	154±25		10
183		163±		180±2				148±
5	39590	22	39577	3	39553	161±24		8
184		148±		147±2				166±
5	39591	20	39578	1	39554	157±20		8
185		142±		112±2				
5	39592	20	39579	0	39555	157±19		
186		140±		128±2				
5	39593	22	39580	1	39556	124±21		
187		126±		140±2				
5	39594	23	39581	0	39557	162±20		
188		132±		166±1				
5	39595	22	39582	9	39558	141±20		
189		114±		117±2				
5	39596	20	39583	0	39559	127±19		
190		106±		117±2			138±2	
5	39597	21	39584	0	39560	130±21	39602	2
191	39598,410	130±		104±1				140±2
5	47*	14	39585	3	41046*	139±24	39603	0
192	41049*	153±		140±2	39562,			167±2
5		20	39586	1	41048*	148±14	39604	2
193	39600,410	168±		166±2	41050*			170±2
5	51*	15	40118	1		177±20	39605	2
194	41053*	164±		187±1	41052*		39606	211±1
5		20	40119	3		155±20		2

Table 2: Calculated regional radiocarbon (^{14}C yrs $\pm 1\sigma$) offsets across common periods.

Time period	Lake Tay (Western Australia), 33°S	Takapari (North Island NZ), 40°S	Dough Boy (Stewart Island), 47°S	Campbell Island (Southern Ocean), 53°S	Tierra del Fuego (S. America), 54°S
1700-1850	57.0 \pm 6.0	37.7 \pm 5.7	44.4 \pm 5.9		38.0 \pm 2.6
1850-1950	17.5 \pm 6.5	15.3 \pm 6.2	25.0 \pm 6.6	30.2 \pm 9.3	
1700-1950	39.0 \pm 4.4	26.7 \pm 4.2	35.0 \pm 4.4		

Accepted Article